A quantum perturbative pair distribution for determining interatomic potentials from extended x-ray absorption spectroscopy

A quantum perturbative pair distribution for determining interatomic potentials from extended x-ray absorption spectroscopy

F Piazza

INFM-UdR Firenze, Via G. Sansone 1, 50019 Sesto F.no (FI), Italy

Abstract

In this paper we develop a technique for determining interatomic potentials in materials in the quantum regime from single-shell extended x-ray absorption spectroscopy (EXAFS) spectra. We introduce a pair distribution function, based on ordinary quantum time-independent perturbation theory. In the proposed scheme, the model potential parameters enter the distribution through a fourth-order Taylor expansion of the potential, and are directly refined in the fit of the model signal to the experimental spectrum. We discuss in general the validity of our theoretical framework, namely the quantum regime and perturbative treatment, and work out a simple tool for monitoring the sensitivity of our theory in determining lattice anharmonicities based on the statistical F-test. As an example, we apply our formalism to an EXAFS spectrum at the Ag K edge of AgI at $T = 77$ K. We determine the Ag–I potential parameters and find good agreement with previous studies.

1. Introduction

It is well known that extended x-ray absorption spectroscopy (EXAFS) is a very sensitive and accurate technique for probing the structural and dynamical properties of materials in the neighbourhood of the photoabsorber atom [1]. In particular, the damping of the EXAFS signal induced by thermal broadening in the distribution of absorber–neighbour distances carries quantitative information on the corresponding interatomic potentials [2].

The effects of thermal disorder are usually accounted for by introducing a temperature-dependent pair distribution function (PDF) $g(r, T)$, such that $g_s(r, T) \, dr$ is the normalized probability that the distance of an atom in the the sth shell from the absorber lies in the interval $[r, r+dr]$ at the temperature T. The corresponding single-shell EXAFS $\chi_s(k)$ is then obtained as

$$\chi_s(k) = \int_0^\infty g_s(r, T) \chi_s(k, r) \, dr. \tag{1}$$

It is clear that the absorber–neighbour effective potential determines the shape of the PDF. The simplest structural model one can introduce is represented by a Gaussian distribution, i.e. a harmonic interatomic potential. In this case, integration of equation (1) is straightforward and the result is the well known Debye–Waller multiplicative damping factor $e^{-2\sigma^2 k^2}$, where $\sigma^2 = \langle [r - \langle r \rangle]^2 \rangle = \int_0^\infty g(r, T)[r - \langle r \rangle]^2 \, dr$.

The higher-order terms in the potential expansion are usually accounted for via the cumulant method [3]. The cumulants C_n are defined as the coefficients that enter the MacLaurin expansion of the function $\ln[F(2k)]$, where $F(2k)$ is the Fourier transform of the effective distribution function $G(r, \lambda) = g(r)e^{-2r/\lambda}/r^2$, λ being the photoelectron mean free path. The utility of this method is that the cumulants are related to the moments of the effective distribution. In particular, the first cumulant C_1 is the mean value of the interatomic distance, while C_2 is the variance of the effective distribution. The higher-order cumulants C_3 and C_4 are related to the *skewness* (asymmetry) and *kurtosis* (deviation from the Gaussian shape) of the distribution, respectively. The cumulant-expansion technique has been applied successfully in the case of moderate anharmonicities both to bulk materials [4] and to the study of surfaces [5, 6].

In such a framework, the following step towards a detailed understanding of disordered systems is to establish the direct relationship between the interatomic potential and cumulants. In the case of harmonic crystals, the second-order cumulants have been calculated quantum mechanically for Debye crystals [7] and simple molecules [8]. Other attempts in this direction exist in the literature which include third-order anharmonicities for simple systems [9, 10].

A more straightforward alternative approach is to directly integrate the EXAFS by calculating explicitly the whole PDF corresponding to a certain model potential. The simplest way a pair potential $V(r)$ may directly enter the distribution function is through the classical configurational integral scheme

$$g(r, T) = \frac{e^{-V(r)/k_B T}}{\int_0^\infty e^{-V(r)/k_B T} \, dr} \qquad (2)$$

where k_B is the Boltzmann constant. Expression (2) has been applied to the study of metals and ionic systems with different model potentials, from Lennard-Jones [11] and Morse [12] to generic three-parameter Taylor expansions [13]. However, equation (2) is based on a classical treatment of the atomic vibrations. In general, depending both on the temperature and potential stiffness, the classical approximation may break down. In this case the full quantum treatment of lattice dynamics is in order, and one can proceed as follows.

First the Schrödinger equation of the absorber–neighbour pair has to be solved, and the eigenvectors ψ_n and eigenvalues E_n computed. The quantum mechanical analogue of expression (2) can then be written as

$$g(r, T) = \frac{\sum_n |\psi_n(r)|^2 e^{-E_n/k_B T}}{\sum_n e^{-E_n/k_B T}}, \qquad (3)$$

where $r = |\boldsymbol{x}_1 - \boldsymbol{x}_2|$ is the spatial coordinate describing the relative motion of the pair. Equation (3) was first introduced and used in [14] to study the interatomic potential of the Cu–O(4) pair in the YBCO superconductor. The procedure is the following: one first introduces a model potential which is characterized by a set of parameters $\{\lambda\}$. Then a numerical routine is set up, which solves the radial Schrödinger equation for a particular choice of the set $\{\lambda\}$, builds the radial distribution function (3) and calculates the EXAFS signal $\chi(k, \{\lambda\})$. This routine is then incorporated in the fitting program that refines the free parameters $\{\lambda\}$ on a set of experimental data through ordinary χ^2 minimization.

This procedure has the advantage that it allows an arbitrary analytical potential function to be used. This is the case of [14], where a double-well potential is found. However, it is rather

cumbersome and of little practical utility for routine fittings. In particular, a more concise and handy way of calculating expression (3) in a closed form would be of great advantage.

In this paper we compute an analytical expression for the function (3), based on a simple Taylor expansion of the potential function, and cast it in a simple form, suitable for inclusion in a simple routine attached to the fitting machinery. We organize our paper as follows. In section 2 we develop our quantum pair distribution function (QPDF). In section 3 we discuss on general grounds the validity of our theoretical framework. Furthermore, we develop a statistical tool to assess the sensitivity of the QPDF to the parameters describing the anharmonicities in the potential. Finally, in section 4 we test the QPDF by fitting an EXAFS spectrum of AgI at $T = 77$ K. We end the paper by summarizing our results and drawing our conclusions in section 5.

2. The quantum pair distribution function

Let us consider the pair formed by the photoabsorber and one of its neighbours from a given coordination shell. Let x_i and m_i $(i = 1, 2)$ denote the position vectors and atomic masses of the two atoms, respectively. Let $V(r)$ be the corresponding interatomic potential. We can write its Taylor expansion in the following fashion:

$$V(r) = \tfrac{1}{2}k_2(r - r_0)^2 + V_1(r) + \mathcal{O}(|r - r_0|^5),\tag{4}$$

where

$$V_1(r) = \tfrac{1}{3}k_3(r - r_0)^3 + \tfrac{1}{4}k_4(r - r_0)^4 \qquad \text{and} \qquad k_m = \frac{1}{(m-1)!}\left[\frac{\mathrm{d}^m V(r)}{\mathrm{d}r^m}\right]_{r=r_0},\tag{5}$$

r_0 being the equilibrium interparticle distance, given by the condition $[\mathrm{d}V(r)/\mathrm{d}r]_{r=r_0} = 0$. We can follow the ordinary procedure to first separate the two-body Schrödinger equation by introducing the relative and centre-of-mass coordinates, and then decouple the angular and radial degrees of freedom in the Schrödinger equation for the radial motion. The pair wavefunction then reads

$$\Psi(x_1, x_2) = \psi_G(X)\left[\frac{u(r)}{r}\right]Y_l^m(\theta, \phi),\tag{6}$$

where $X = (m_1 x_1 + m_2 x_2)/(m_1 + m_2)$, $r = |x_1 - x_2|$ and $Y_l^m(\theta, \phi)$ are the spherical harmonic functions [15]. We require the wavefunction of the pair to have spherical symmetry, since we do not want the PDF to depend on the orientation of the absorber–neighbour bond in the crystal[1]. We therefore set $l = 0$. The radial equation then reduces to the one-dimensional problem

$$-\frac{\hbar^2}{2\mu}\frac{\mathrm{d}^2 u}{\mathrm{d}r^2} + \left[\frac{1}{2}k_2(r - r_0)^2 + V_1(r)\right]u = Eu,\tag{7}$$

where μ is the reduced mass of the pair and we require $u(r)|_{r=0} = 0$. In the spirit of ordinary time-independent perturbation theory, we consider the harmonic Hamiltonian as the unperturbed problem and the potential V_1 as the perturbation.

It is convenient to adopt the formalism of second quantization. The unperturbed problem is defined by the eigenvectors $|n\rangle$ and the corresponding eigenvalues $E_n^{(0)} = \hbar\omega[n + 1/2](n = 0, 1, 2, \ldots)$, where $\omega = \sqrt{k_2/\mu}$. Recalling the well known commutation relations between creation and annihilation operators $\hat{a}^\dagger$ and $\hat{a}$, respectively, it is straightforward to write down

---

[1] This also means that our formalism in its present form only applies to the study of K edges.

the expression of the perturbation potential (5) in the n-representation. We get

$$\mathcal{V} = \hbar\omega\,\Lambda_3[\hat{a}^{\dagger 3} + \hat{a}^3 + 3n\hat{a}^\dagger + 3(n+1)\hat{a}] \tag{8}$$
$$+ \hbar\omega\Lambda_4[\hat{a}^{\dagger 4} + \hat{a}^4 + 2(2n-1)\hat{a}^{\dagger 2} + 2(2n+3)\hat{a}^2 + 3(n+1)^2 + 3n^2],$$

where

$$\Lambda_m = \frac{1}{2^{m/2}m}\left(\frac{k_m x_0^m}{\hbar\omega}\right) \qquad (m = 3, 4) \text{ and } x_0 = \sqrt{\hbar/\mu\omega}. \tag{9}$$

Recalling the definition of creation and annihilation operators we can easily evaluate the matrix elements $\langle k|\mathcal{V}|n\rangle$. Let us define the four-dimensional quantity β as

$$\beta(\sigma) = \Lambda_3[\delta_{\sigma,1} + \delta_{\sigma,3}] + \Lambda_4[\delta_{\sigma,2} + \delta_{\sigma,4}] \qquad (\sigma = 1, 2, 3, 4), \tag{10}$$

where $\delta_{i,j}$ is the Kronecker integer delta function. We get

$$\langle k|\mathcal{V}|n\rangle = \langle n|\mathcal{V}|k\rangle = \sum_{\sigma=1}^{4}\beta(\sigma)[\gamma_n^+(\sigma)\delta_{k,n+\sigma} + \gamma_n^-(\sigma)\delta_{k,n-\sigma}], \tag{11}$$

where we have explicitly used the hermiticity of $\mathcal{V}$, and defined

$$\gamma_n^+(\sigma) = \sqrt{\frac{(n+\sigma)!}{n!}}\alpha^+(n,\sigma) \qquad \gamma_n^-(\sigma) = \begin{cases} \sqrt{\dfrac{n!}{(n-\sigma)!}}\alpha^-(n,\sigma) & n \geqslant \sigma \\ 0 & \text{otherwise.} \end{cases} \tag{12}$$

The coefficients $\alpha^\pm(n,\sigma)$ are reported in table 1. We note that the coefficients γ_n and $\alpha^\pm(n,\sigma)$ satisfy the following relations:

$$\begin{aligned} \gamma_{n-\sigma}^+(\sigma) &= \gamma_n^- & \alpha^+(n-\sigma,\sigma) &= \alpha^-(n,\sigma) \\ \gamma_{n+\sigma}^-(\sigma) &= \gamma_n^+ & \alpha^-(n+\sigma,\sigma) &= \alpha^+(n,\sigma). \end{aligned} \tag{13}$$

Using equations (11)–(13), we can work out the second-order corrections to the energy levels ΔE_n and the normalized perturbed wavefunctions $|n\rangle + |n'\rangle$ in the usual way (see e.g. [16]). After a somewhat lengthy calculation, we get

$$\Delta E_n/\hbar\omega = 3\Lambda_4(2n^2 + 2n + 1) + \sum_{\sigma=1}^{4}\frac{\beta(\sigma)^2}{\sigma}[(\gamma_n^-(\sigma))^2 - (\gamma_n^+(\sigma))^2] \tag{14}$$

$$\begin{aligned} |n'\rangle = &\sum_{\sigma=1}^{4}\frac{\beta(\sigma)}{\sigma}[\gamma_n^-(\sigma)|n-\sigma\rangle - \gamma_n^+(\sigma)|n+\sigma\rangle] \\ &+ \sum_{\sigma,\sigma'=1}^{4}\frac{\beta(\sigma)\beta(\sigma')}{\sigma(\sigma+\sigma')}[\gamma_n^+(\sigma)\gamma_{n+\sigma}^+(\sigma')|n+(\sigma+\sigma')\rangle \\ &+ \gamma_n^-(\sigma)\gamma_{n-\sigma}^-(\sigma')|n-(\sigma+\sigma')\rangle] \\ &- \sum_{\sigma\neq\sigma'=1}^{4}\frac{\beta(\sigma)\beta(\sigma')}{\sigma(\sigma'-\sigma)}[\gamma_n^+(\sigma)\gamma_{n+\sigma}^-(\sigma')|n-(\sigma'-\sigma)\rangle \\ &+ \gamma_n^-(\sigma)\gamma_{n-\sigma}^+(\sigma')|n+(\sigma'-\sigma)\rangle] \\ &- \frac{\Delta E_n^{(1)}}{\hbar\omega}\sum_{\sigma=1}^{4}\frac{\beta(\sigma)}{\sigma^2}[\gamma_n^+(\sigma)|n+\sigma\rangle + \gamma_n^-(\sigma)|n-\sigma\rangle] \\ &- \frac{1}{2}|n\rangle\sum_{\sigma=1}^{4}\frac{\beta^2(\sigma)}{\sigma^2}[(\gamma_n^+(\sigma))^2 + (\gamma_n^-(\sigma))^2], \end{aligned} \tag{15}$$

Table 1. Values of the coefficients $\alpha^{\pm}(n, \sigma)$.

σ	$\alpha^{+}(n, \sigma)$	$\alpha^{-}(n, \sigma)$
1	$3(n + 1)$	$3n$
2	$2(2n + 3)$	$2(2n - 1)$
3	1	1
4	1	1

where $\Delta E_n^{(1)} = 3\hbar\omega\Lambda_4(2n^2 + 2n + 1)$ are the first-order corrections to the energy levels.

We are now able to write down explicitly the expression for the QPDF from equation (3). We have

$$g(r, T) = \frac{\sum_{n=0}^{n_M}[u_n(r) + u'_n(r)]^2 e^{-[E_n^{(0)}+\Delta E_n]/k_B T}}{\sum_{n=0}^{n_M} e^{-[E_n^{(0)}+\Delta E_n]/k_B T}}, \qquad (16)$$

where $u_n(r) = \langle r|n\rangle$ are the unperturbed eigenfunctions, i.e. the eigenvectors of the one-dimensional harmonic oscillator, and $u'_n(r) = \langle r|n'\rangle$ are the corrections (15). We have explicitly indicated the truncation of the summations as the integer n_M. In the computations one has to fix n_M by requiring that the corresponding normalized Boltzmann factor z_{n_M}/Z (Z being the partition function) is negligible up to some specified tolerance tol $= 10^{-M}$, i.e.

$$z_{n_M} = e^{-[E_{n_M}^{(0)}+\Delta E_{n_M}]/k_B T} \leqslant \text{tol}. \qquad (17)$$

This condition fixes the number of levels which are included in the perturbative series (16). Of course, one also has to check that the energy of the highest level included is small compared to some estimate of the potential well depth V_o. If we express energies in eV and temperature in Kelvin, from equation (17) we get the condition

$$[M \log 10]T \times 10^{-4} < V_o. \qquad (18)$$

It follows that, for potential well depths of the order of 1 eV, the condition (18) is fulfilled for $M = 4$–5 for temperatures up to ≈ 100 K.

3. Validity and sensitivity of the QPDF

The above described procedure to build the QPDF relies on two basic hypotheses:

(i) the classical approximation of lattice vibrations must be inadequate so that the quantum treatment of the two-body problem holds, and

(ii) the deviations of the absorber–neighbour potential from the harmonic approximations must be satisfactorily described by a perturbative treatment.

As to the validity of condition (i), the ratio $\mathcal{R}_Q = \hbar\omega/k_B T$ ($\omega = \sqrt{k_2/\mu}$) provides a good qualitative indicator: if $\mathcal{R}_Q$ is of the order of unity, the quantum energy scale is comparable with the thermal one, and the system requires the full quantum description. Regarding condition (ii), we introduce the following parameter:

$$\mathcal{R}_E \stackrel{def}{=} \frac{2V_1(\sqrt{\langle(r - r_0)^2\rangle_T})}{k_2\langle(r - r_0)^2\rangle_T} = \frac{1}{k_2}\left[\frac{2}{3}k_3\sqrt{\langle(r - r_0)^2\rangle_T} + \frac{1}{2}k_4\langle(r - r_0)^2\rangle_T\right], \qquad (19)$$

where $\langle\ldots\rangle_T$ is the configurational average performed with the QPDF. The indicator $\mathcal{R}_E$ gives a measure of the relative strength of the perturbed and unperturbed energies, and can always be computed *a posteriori* in order to assess the validity of the perturbative approximation. On the other hand, we also have to be concerned with the *sensitivity* of the QPDF to the parameters

of the model potential. i.e. the minimum detectable anharmonicity within the present model at fixed temperature and potential stiffness (k_2). We shall here introduce a simple procedure for assessing the QPDF sensitivity, based on the statistical F-test.

Let us suppose that we are fitting N experimental data points (k_i, χ_i^{exp}), $i = 1, \ldots, N$, to a model that has p adjustable parameters λ_j, $j = 1, \ldots, p$. The model predicts a functional relationship between the measured independent and dependent variables

$$\chi(k) = \chi^{the}(k; \lambda_1, \ldots, \lambda_p).$$

In the spirit of the maximum-likelihood method, we want to minimize a fit index (or residual function) of the kind

$$\mathcal{F} = \sum_{i=1}^{N} [\chi_i^{exp} - \chi^{the}(k_i; \lambda_1, \ldots, \lambda_p)]^2 w_i \tag{20}$$

where the w_i are some weight functions. In general, if the standard deviations σ_i of the experimental data are known independently, the correct choice would be $w_i \propto 1/\sigma_i^2$. However, depending on the particular algorithm used to perform the fit, some other weighting functions may be preferred.

As a consequence of introducing the third- and fourth-order nonlinearities in the model potential, two more floating parameters are available to fit the EXAFS spectrum, namely k_3 and k_4. In general, this will cause *per se* a reduction of the best-fit index minimum with respect to the harmonic model. Such a situation typically arises in EXAFS data analysis when it is to be decided whether a spectrum needs the introduction of an additional shell to be fitted (some physical information still present in the data) or, more generally, whether the improvement achievable by incrementing the number of free parameters is statistically meaningless [17, 18]. In our case, we are interested in assessing the sensitivity of the QPDF in capturing real physical information regarding the higher-order terms in the Taylor expansion of the potential.

A general theorem in statistics states that the minimum of the residual function $\mathcal{F}_{min}$ is distributed as a χ^2 distribution with $\nu_1 = N - (p + 1)$ degrees of freedom [19][2]. Let us assume we want to compare an harmonic model potential (fit with p parameters) to a potential obtained by adding some anharmonicity (fit with $p + p'$ parameters, $p' = 1, 2$). We want to assess whether the latter model *significantly* improves the fit (given the automatic improvement following the introduction of any additional free parameter). Let us consider the ratio of the normalized minima of the two corresponding fit indices

$$F = \frac{\mathcal{F}_{min}(p)/\nu_1}{\mathcal{F}_{min}(p + p')/\nu_2}, \tag{21}$$

where $\nu_2 = [N - (p + p' + 1)]$. It can be shown that, as a consequence of the above theorem, the ratio (21) follows an F_{ν_1,ν_2} distribution [19], whose density function is

$$\mathcal{D}_{\nu_1,\nu_2}(F)\,\mathrm{d}F = \frac{\Gamma[(\nu_1 + \nu_2)/2][(\nu_1/\nu_2)F]^{\nu_1/2 - 1}}{\Gamma(\nu_1/2)\Gamma(\nu_2/2)[(\nu_1/\nu_2)F + 1]^{(\nu_1 + \nu_2)/2}}\,\mathrm{d}F. \tag{22}$$

In particular, if both the harmonic and anharmonic models were appropriate to explaining all of the signal, one would expect the function

$$f = \frac{\nu_2}{p'}\left(\frac{\mathcal{F}_{min}(p)}{\mathcal{F}_{min}(p + p')} - 1\right) \tag{23}$$

---

[2] This result strictly holds when (i) the measurement errors are normally distributed, and either (ii) the model is linear in its parameters or (iii) the sample size is large enough that the uncertainties in the fitted parameters do not extend outside a region in which the model could be replaced by a suitable linearized model. Fits in EXAFS are usually at the limit of validity of condition (iii). However, all the statistical analysis that stems from this basic theorem is routinely applied in EXAFS data analysis (see e.g. [20]).

to follow an F_{p', ν_2} distribution. The F-test is then conducted as follows.

(1) Based on some estimate of the experimental standard deviation, one generates an *artificial* experimental data set from the anharmonic model, e.g. by adding some Gaussian noise.
(2) The two residuals $\mathcal{F}_{min}(p)$ and $\mathcal{F}_{min}(p + p')$ are calculated and the value of f obtained.
(3) One can now fix the preferred confidence level c and compare f with F^c_{p', ν_2}, given by the following relation:

$$c = 1 - \int_0^{F^c_{p', \nu_2}} \mathcal{D}_{p', \nu_2}(F) \, \mathrm{d}F. \tag{24}$$

Here c is the percentage probability of obtaining a reduction $\mathcal{F}_{min}(p) - \mathcal{F}_{min}(p + p')$ as large as actually observed, when the added anharmonicity is not physically meaningful. We shall call such a confidence level the *rejection probability*, which expresses the probability that the harmonic and anharmonic model are equivalent—that is, if $c = 1$ the two models are by all means statistically indistinguishable, while if $c = 0$ the probability that the harmonic model could explain the data instead of the anharmonic one vanishes identically.

4. The Ag–I potential in silver iodide

Silver iodide (AgI) is known for being a highly anharmonic material [21–23]. Hence, it appears a good candidate for providing a bench-mark to test the above described data analysis framework. As an example, we analyse here an Ag K-edge EXAFS spectrum collected at $T = 77$ K. The details of the experiment and of the extraction of the EXAFS signal $\chi^{exp}(k)$ from the raw absorption data are reported elsewhere [25].

The classical expression (2) of the PDF has been recently used in an EXAFS study of AgI at the I K edge to measure the first three coefficients of the Taylor expansion of the Ag–I potential at $T = 300$ and 600 K [24]. Following [24], we get $\mathcal{R}_Q(T = 77) \approx 0.5$. We conclude that at $T = 77$ K the classical expression of the PDF is no longer valid and one has to work in the quantum regime. In order to calculate the model EXAFS signal we re-write equation (1) by using the standard formula of single-shell single-scattering EXAFS in the following fashion:

$$\chi(k, r) = S_o^2 N_I \int_{-\infty}^{+\infty} g(u, T) \frac{\mathrm{e}^{-2[r_0 + u]/\lambda(k)}}{k[r_0 + u]^2} \mathrm{Im}\{ f_I(\pi, k) \mathrm{e}^{2\mathrm{i}\delta_{Ag}} \mathrm{e}^{2\mathrm{i}k[r_0 + u]} \} \, \mathrm{d}u, \tag{25}$$

where $g(u, T)$ is the QPDF as calculated from equation (16) and we have made the substitution $u = r - r_0$. Here N_I is the coordination number of the I ions, which we fixed at the crystallographic value $N_I = 4$, δ_{Ag} is the central atom phase shift and $f_I(\pi, k) = |f_I(\pi, k)| \exp(\mathrm{i}\phi_I)$ is the complex backscattering amplitude of the I ions. The constant S_o^2 is the usual reduction factor which accounts for the inelastic losses, which we fixed at the value $S_o^2 = 0.73$ [25]. The photoelectron mean free path is here assumed to depend on the wavevector k as $\lambda = k/\eta$ [2], where η is a constant. The backscattering amplitude $f_I(\pi, k)$ and total phase shift $\Delta\varphi = 2\delta_{Ag} + \phi_I$ have been taken from the tables in [2] (reproduced from calculations based on the Herman–Skillman wavefunctions [26]).

Following the arguments developed in section 3, we carry out two separate non-linear least-squares fittings, by comparing the experimental EXAFS $\chi^{exp}(k)$ with the model signal calculated by equation (25) from the two separate sets of floating parameters $\{\lambda\} = \{r_0, \Delta E_0, \eta, k_2\}$ and $\{\lambda'\} = \{r_0, \Delta E_0, \eta, k_2, k_3, k_4\}$. The floating parameter ΔE_0 must be included in the fit as usual in order to compensate for the uncertainty associated with the *true* value of the threshold energy, i.e. the minimum energy required to free the photoelectron.

(a)

(b)
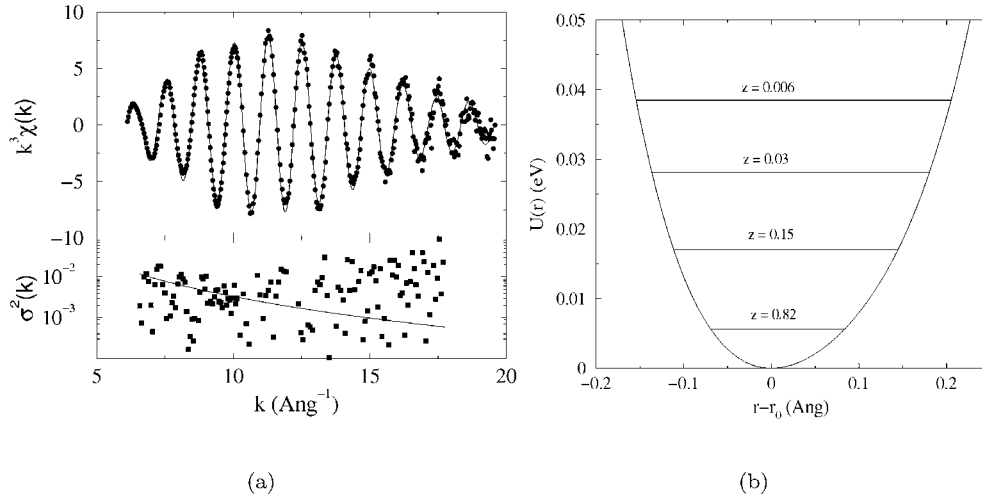
Figure 1. (a) Upper frame: Ag K-edge EXAFS signal at $T = 77$ K (symbols) and fit obtained with equation (25) and parameter set $\{\lambda'\}$. Lower frame: squared residuals (symbols) and fit with the law $\sigma^2(k) = \sigma_0^2 [k_0/k]^3$ (solid curve). Units for the y-axis are Å^2. (b) Effective Ag–I potential. Also shown are the harmonic levels used to calculate the QPDF, and the corresponding normalized Boltzmann factors z_n/Z.

Table 2. Best-fit values of the fit index (20) and parameters describing the Ag–I potential. The weight functions used are here $w_i = 1/\sqrt{50}\forall i$.

Model	$\mathcal{F}_{min}$	k_2 (eV Å^{-2})	k_3 (eV Å^{-3})	k_4 (eV Å^{-4})	η (Å^{-2})	r_0 (Å)	ΔE_0 (eV)
$\{\lambda\}$	41.0	2.11(3)	—	—	0.84(5)	2.86(1)	−48(1)
$\{\lambda'\}$	31.5	1.86(3)	−7.6(4)	49(6)	0.82(5)	2.87(1)	−43(1)

Table 3. Ag–I potential parameters as measured in [24].

| T (K)	k_2 (eV Å^{-2})	k_3 (eV Å^{-3})	k_4 (eV Å^{-4})
300	2.4(1)	−5.0(1)	0.2(0.7)
600	2.7(1)	−5.3(1)	0.08(0.4)

The best-fit values of the free parameters are reported in table 2 for both the harmonic and anharmonic models, alongside with the corresponding fit index minimum $\mathcal{F}_{min}$. The quality of the fit with the anharmonic model is shown in figure 1(a), while the corresponding effective Ag–I potential is drawn in figure 1(b). In table 3 we report for comparison the values of the potential parameters as measured in [24]. We see that the overall agreement is good, although the value of k_4 reported in [24] does not seem to be reliable. Moreover, if we use equation (19) to estimate the strength of the perturbation energy corresponding to the best-fit values of k_3 and k_4, we get $\mathcal{R}_E \approx 0.12$. We conclude that our results of the analysis with the QPDF are consistent with the perturbative hypothesis. It is instructive to observe that the same analysis performed using the classical expression of the PDF equation (2) with the parameter set $\{\lambda'\}$ always yields a vanishing k_2 at the minimum $\mathcal{F}_{min}$. Correspondingly, the fourth-order constant k_4 is raised to unphysically high values, independently of the initial guess of the set $\{\lambda'\}$. This scenario clearly confirms the inadequacy of the classical treatment of the pair dynamics in the present case.
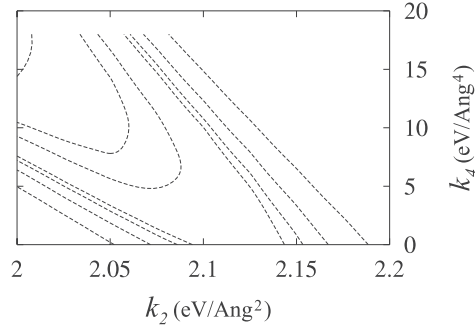
Figure 2. Contour levels of the function $\Delta\mathcal{F} = \mathcal{F}(k_2, k_4) - \mathcal{F}_{min}$ for the minimum corresponding to the harmonic model. The contours correspond, from left to right, to $\Delta\mathcal{F} = -[\chi^2]^{0.01}_{\nu=2}, -[\chi^2]^{0.1}_{\nu=2}, -[\chi^2]^{0.3}_{\nu=2}, [\chi^2]^{0.5}_{\nu=2}, [\chi^2]^{0.3}_{\nu=2}, [\chi^2]^{0.1}_{\nu=2}$ and $[\chi^2]^{0.01}_{\nu=2}$.

We turn now to assessing the validity of our treatment on statistical grounds. The value of f corresponding to the reduction of $\mathcal{F}$ following the introduction of k_3 and k_4 can be calculated by equation (23). Substituting $N = 150$ and $p' = 2$, we get $f \approx 16.6$. By substituting in turn $F^c_{p', \nu_2} = f$ in equation (24) we get the corresponding rejection probability $c \approx 3 \times 10^{-7}$. We are then allowed to conclude that the anharmonic model is here capturing a real physical feature of the Ag–I pair dynamics. It is instructive to demonstrate this conclusion in a more pictorial fashion. It is a simple corollary to the first theorem mentioned in section 3 that, if only ν parameters are varied while keeping the other $p-\nu$ fixed at their best-fit value, the function $\Delta\mathcal{F} = \mathcal{F}(\lambda_1, \lambda_2, \ldots, \lambda_\nu) - \mathcal{F}_{min}$ follows a χ^2 distribution with ν degrees of freedom. When $\nu = 2$ this result provides the errors on selected parameter pairs (λ_1, λ_2) in the form of *confidence ellipses* through the simple condition $\Delta\mathcal{F}(\lambda_1, \lambda_2) = [\chi^2]^c_{\nu=2}$. Here $[\chi^2]^c_{\nu=2}$ is the value of the χ^2 variable corresponding to the required confidence level (i.e. rejection probability) c for $\nu = 2$. In figure 2 we show the contour levels of the function $\Delta\mathcal{F} = \mathcal{F}(k_2, k_4) - \mathcal{F}_{min}$ computed for the minimum obtained within the harmonic model. The presence of a significant region (corresponding to the 99% confidence level $[\chi^2]^{0.01}_{\nu=2} = 9.21$) of negative values away from the computed minimum explains the dramatic improvement of the fit upon introducing the nonlinearities in the potential. The same confidence analysis for the anharmonic model performed in four different parameter subspaces $\{\lambda_1, \lambda_2\}$ is reported in figure 3, showing the quality of the best-fit minimum.

We end this section by showing how one can conduct the F-test described in section 3 to examine the QPDF sensitivity in the present case. Let us fix the temperature and the harmonic constant k_2 at its best-fit value. We can then use equations (20), (23) and (25) with $p' = 1$ to calculate the value of f for any choice of k_3 and k_4, where in place of the experimental spectrum we use an artificial data set constructed as described in section 3. In particular, we just add to the model signal a Gaussian noise with standard deviation $\sigma(k, T) = \sigma_0 [k_0/k]^{3/2}\sqrt{T/T_0}$, with $\sigma_0^2 = 0.0016$, $k_0 = 12.7$ Å^{-1} and $T_0 = 77$ K (see figure 1(a)). Finally, we calculate the corresponding rejection probability by means of equation (24) with $F^c_{p', \nu_2} = f$. For example, this procedure can be used to construct the functions $c(k_3, k_4 = 0, T)$ and $c(k_3 = 0, k_4, T)$ (one-parameter sensitivity curves). Alternatively, the same procedure with $p' = 2$ can be used to look at the contour sections of the function $c(k_3, k_4, T)$ (two-parameter sensitivity curves). In figure 4 we show an example of one-parameter sensitivity curves calculated at three different temperatures for both the k_3 and k_4 parameters. We clearly see that the lowest detectable anharmonicity is well below the measured one in both cases. In particular, the rejection probability decays exponentially with increasing magnitude of the anharmonic constant.
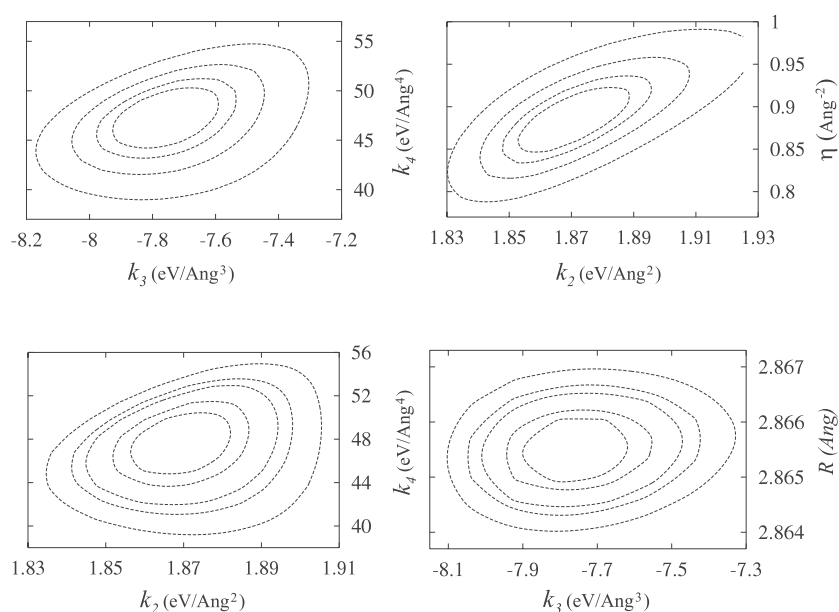
Figure 3. Contour levels of the function $\Delta\mathcal{F} = \mathcal{F}(\lambda_1, \lambda_2) - \mathcal{F}_{min}$ for the minimum corresponding to the anharmonic model. Four combinations of floating parameter pairs $\{\lambda_1, \lambda_2\}$ are shown. Contours correspond to confidence levels 50%, 70%, 90%, (95%) and 99%.
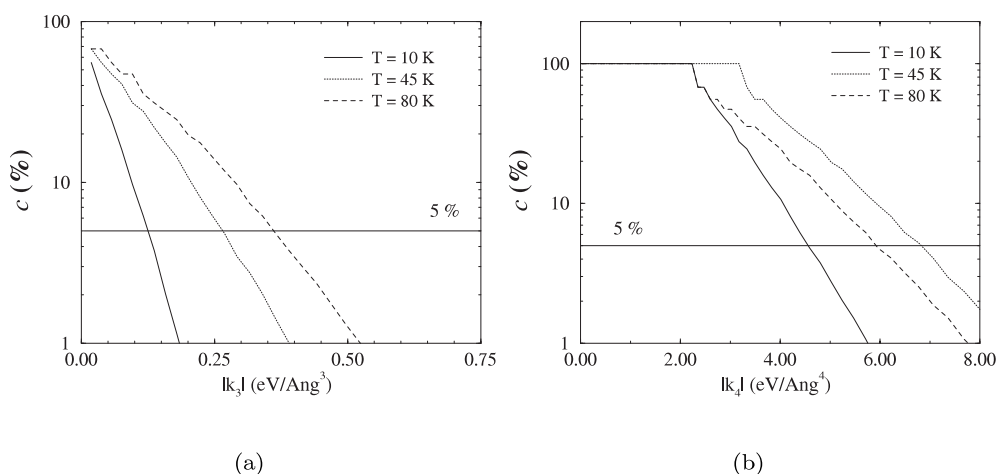
Figure 4. Rejection probability as a function of the potential anharmonicity calculated by equation (24) at different temperatures for fixed harmonic constant. Parameters are $N = 150$, $\mu = 9.74 \times 10^{-26}$ kg and $k_2 = 1.86$ eV Å^{-2}. (a) Cubic nonlinearity; (b) quartic nonlinearity.

5. Conclusions

In this paper we have introduced a PDF valid in the quantum regime based on a Taylor expansion of the absorber–neighbour potential, suitable for the analysis of single-scattering EXAFS. In particular, we used ordinary time-independent non-degenerate quantum perturbation theory to cast the QPDF in a simple analytical form, which can be easily calculated in a subroutine

incorporated in the fitting program. Moreover, we have shown how the limits of validity (sensibility of the quantum treatment and perturbative hypothesis) can be monitored and described how to implement a simple statistical test to estimate the sensitivity of the QPDF to the third- and fourth-order terms in the potential. The latter procedure can be used *a posteriori* to check whether the best-fit values of the anharmonic parameters are above the sensitivity level (minimum detectable anharmonicity). Alternatively, the same procedure may be applied *a priori* in order to assess whether the QPDF is suitable for the analysis of the problem at hand. We applied our formalism to the case of AgI, showing how the potential anharmonicity can be measured in a temperature range where the classical expression of the PDF could not be used. In particular, we demonstrated how a simple harmonic model is not adequate to describing the dynamics of the Ag–I pair, in agreement with previous studies performed in the classical regime.

As a final remark, it should be noted that the example we chose to test the QPDF concerns a very symmetric lattice structure. It is well known that an additional broadening of the distributions of absorber–neighbour distances may be produced by static disorder. The latter may be associated for example with the presence of a coordination shell made of N identical atoms at slightly different distances from the photoabsorber, that cannot be resolved in different subshells (e.g. N_1 at distance r_1 and N_2 at distance r_2, with $N_1 + N_2 = N$). For small static disorder ($|r_1 - r_2| \ll r_1, r_2$), one can prove that such shell is equivalent to a shell with coordination N and mean distance $r_0 = (N_1 r_1 + N_2 r_2)/N$, provided one introduces in the Debye–Waller factor the additional variance $\sigma_{\text{stat}}^2 = N_1 N_2 |r_1 - r_2|^2/N^2$ [2]. In the framework of our model, this is expected to correspondingly rescale the harmonic constant k_2. However, it should not alter in general the information carried by the EXAFS signal regarding the anharmonic terms of the absorber–neighbour effective potential. Hence, we expect that our model of lattice anharmonicities may be sensibly used in its present form also in the presence of small static disorder.

Concluding, we have developed an easy technique to study interatomic potentials from single-scattering EXAFS in the quantum regime of atomic vibrations. A full-featured FORTRAN package containing the relevant programs is made available by the author to interested scientists upon request.

Acknowledgments

References

[1] Konïngsberger D C and Prins R (ed) 1988 *X-Ray Absorption: Principles, Applications, Techniques of EXAFS, SEXAFS and XANES* (New York: Wiley)
[2] Teo B K 1986 *EXAFS: Basic Principles and Data Analysis* (Berlin: Springer)
[3] Bunker G 1983 *Nucl. Instrum. Methods* **207** 437
[4] See, for instance
Yokoyama T and Ohta T 1990 *J. Appl. Phys.* **29** 2052
Tröger L *et al* 1994 *Phys. Rev.* B **49** 888
[5] Yokoyama T *et al* 1994 *Surf. Sci.* **313** 197
[6] Wenzel L, Stöhr J, Arvanitis D and Baberschke K 1988 *Phys. Rev. Lett.* **60** 2327

 [7] Beni G and Platzman P M 1976 *Phys. Rev.* B **14** 1514
 [8] Boland J J and Baldeschwieler 1984 *J. Chem. Phys.* **80** 3005
 [9] Rabus H 1991 *PhD Thesis* Freie Universität Berlin
[10] Frenkel A I and Rehr J J 1993 *Phys. Rev.* B **48** 585
[11] Eisenberger P and Brown G S 1979 *Solid State Commun.* **29** 481
[12] Marques E C, Sandstrom D R, Lytle F W and Greegor R B 1982 *J. Chem. Phys.* **77** 1027
[13] Stern E A, Livins P and Zhang Z 1991 *Phys. Rev.* B **43** 8850
[14] Mustre de Leon J, Conradson S D, Batistić I and Bishop A R 1990 *Phys. Rev. Lett.* **65** 1675
[15] See e.g.
      Winter R G 1986 *Quantum Physics* (Davis, CA: Faculty Publishing)
[16] See e.g.
      Cohen-Tannoudji C, Diu B and Laloe F 1973 *Mechanique Quantique* (Paris: Hermann)
[17] Filipponi A 1995 *J. Phys.: Condens. Matter* **7** 9343
[18] Joyner R W, Martin K J and Meehan P 1987 *J. Phys. C: Solid State Phys.* **20** 4005
[19] See e.g.
      Roe B P 2001 *Probability and Statistics in Experimental Physics* (New York: Springer)
[20] Draper N R and Smith H 1981 *Applied Regression Analysis* (New York: Wiley)
[21] Yoshiasa A, Koto K, Kanamaru F, Emura S and Horiuchi H 1987 *Acta Crystallogr.* B **43** 434
[22] Dalba G, Fornasini P, Rocca F and Mobilio S 1990 *Phys. Rev.* B **41** 9668
[23] Dalba G, Fornasini P and Rocca F 1993 *Phys. Rev.* B **47** 8502
[24] Yoshiasa A and Maeda H 1999 *Solid State Ion.* **121** 175
[25] Ghigna P, Di Muri M, Mustarelli P, Tomasi C and Magistris A 2000 *Solid State Ion.* **136/137** 479
[26] Teo B K and Lee P A 1979 *J. Am. Chem. Soc.* **101** 2815